Available online at www.sciencedirect.com
ScienceDirect
Journal of Organometallic Chemistry 692 (2007) 831–838
Journal of Organometallic Chemistry
www.elsevier.com/locate/jorganchem

A DFT/TDDFT study on the structures, trend in DNA-binding and spectral properties of molecular "light switch" complexes $[Ru(phen)_2(L)]^{2+}$(L = dppz, taptp, phehat)

Jun Li [a], Jin-Can Chen [a], Lian-Cai Xu [a], Kang-Cheng Zheng [a,*], Liang-Nian Ji [a,b,*]

[a] School of Chemistry and Chemical Engineering, The Key Laboratory of Gene Engineering of Ministry of Education, State Key Laboratory of Optoelectronic Materials and Technologies, Sun Yat-Sen University, Guangzhou 510275, PR China
[b] Department of Chemistry, Tongji University, Shanghai 200092, PR China

Received 2 June 2006; received in revised form 2 October 2006; accepted 11 October 2006
Available online 24 October 2006

Abstract

Theoretical studies on a series of molecular "light switch" complexes $[Ru(phen)_2L]^{2+}$ (phen = 1,10-phenanthroline; L: dppz = dipyrido [3,2-*a*:2′,3′-*c*]phenazine; taptp = 4,5,9,18-tetraazaphenanthreno-[9,10-*b*]triphenylene; phehat = 1,10-phenanthrolino[5,6-*b*]1,4,5,8,9,12-hexaazatriphenylene) **1**–**3** have been carried out applying DFT/TDDFT (density functional theory and time-dependent DFT) methods. The geometric and electric structure-characteristics of these complexes have been revealed, and the trend in their DNA-binding constants (K_b), i.e., K_b (**2**) < K_b (**3**) < K_b (**1**), which closely relates to the luminescence properties of the complexes in DNA, has been reasonably explained. The results show that simply increasing the planar area of intercalative ligand may be ineffective on improvement of DNA-binding of resulting complex because of going with the increase in the LUMO (and LUMO + *x*) energy, but introducing some heteroatoms (e.g., N atom) with stronger electronegativity into the ring skeleton of intercalative ligand should be effective because of the decrease in the LUMO (and LUMO + *x*) energy to a certain extent. In addition, the spectra of this series of complexes in vacuo are also computed, simulated, and minutely discussed by the DFT/TDDFT methods, and it is interesting to find that the symmetries of the excited and accepting orbitals of the transition with the largest *f* value are the same.

Keywords: Ru(II) complex; Light switch; DNA-binding; DFT; TDDFT

1. Introduction

The clinical utility of transition metal complexes binding to DNA has inspired a great interest in design and development of such a type of complex that can act as luminescent probes and molecular "light-switches" [1,2]. Ru(II) polypyridyl complexes are therein the most attractive research objects because they possess many excellent performances closely relative to their structures, e.g., the binding to DNA in intercalative but noncovalent mode, the light-absorption and emission in the visible area, the coordinatively saturated but modifiable structures, etc. [3–5]. During the last more than 15 years, $[Ru(phen)_2(dppz)]^{2+}$ and $[Ru(bpy)_2(dppz)]^{2+}$ (bpy = 2,2′-bipyridine) well-known as molecular "light switches" of DNA have induced considerable interest, after the discoveries that they exhibit a negligible background emission in water but exhibit an intense luminescence in the presence of double strand DNA [6,7]. Moreover, their marked luminescence enhancement can owe to their ligand dppz binding to the DNA-base-pairs in intercalative mode [8,9], because the intercalative ligand (dppz) of $[Ru(L)_2(dppz)]^{2+}$(L = phen, bpy) can be protected by the DNA from its interaction with solvent water molecules, resulting in an enormous increase in quantum yield. It is the reason why these complexes possess an excellent molecular "light switch" performance [10–12].

* Corresponding authors. Tel.: +86 20 84110696; fax: +86 20 84112245.
E-mail addresses: ceszkc@sysu.edu.cn (K.-C. Zheng), cesjln@sysu.edu.cn (L.-N. Ji).

0022-328X/$ - see front matter © 2006 Elsevier B.V. All rights reserved.
doi:10.1016/j.jorganchem.2006.10.029

Modifying the polypyridine ligands can usually create some unique differences in the DNA-binding and spectral properties of the resulting complexes [6,13,14]. Therefore, during the last decade, in order to develop novel molecular "light switch" Ru(II) complexes, three main considerations have been presented and performed in experiments: (1) introducing some substituents on the intercalative ligand (dppz) of $[Ru(L)_2(dppz)]^{2+}$(L = phen, bpy) [15,16]; (2) enlarging the conjugate area of the intercalate ligand based on dppz or/and introducing some heteroatoms (e.g., N atom) with stronger electronegativity into the ring skeleton of intercalative ligand [17,18]; (3) developing novel parent ligand as an intercalative ligand, e.g., 2-phenylimidazo[4,5-*f*] [1,10]-phenanthroline (pip) and 2-(4-hydroxyphenyl)imidazo[4,5-*f*] [1,10] phenanthroline (hpip), and so forth [4,19]. In addition to experimental work, many theoretical researchers have tried to correlate the experimental findings with theoretical predictions. Some studies on trends in DNA-binding affinities of this kind of Ru(II) complex applying the density functional theory (DFT) [20–22] method have been reported [23–27]. However, most of them mainly focus on the effects of substituents of intercalative ligand [25–27], including our recent report on the trend in DNA-binding affinitie of complexes $[Ru(bpy)_2(p\text{-}R\text{-}pip)]^{2+}$ (R = –OH, $–CH_3$, –H, $–NO_2$) [28], whereas the DFT studies on the effects of increasing the conjugate area of intercalative ligand as well as introducing some heteroatoms (e.g., N atom) with stronger electronegativity into the ring skeleton of intercalative ligand have not been found yet.

On the other hand, in the last several years, time-dependent density function theory (TDDFT) has become a popular tool for the calculation of various response properties, such as electronic excitations or polarizabilities in medium and large size molecules, due to its good accuracy and reasonable computational cost [29,30]. Although TDDFT still introduces errors by using approximate xc-functional and fails in the excited states for long distance charge transition [31,32], it has been successfully used to calculate the spectral properties of general transition metal complexes [33]. More recently, TDDFT calculations on several ligands and related Ru(II) complexes have also been reported [34–37]. We have also reported some TDDFT studies on spectral properties of Ru(II) polypyridyl complexes [27,28].

Since the DNA-"light switch" behaviors of Ru(II) polypyridyl complexes closely relate to the trend in DNA-binding affinities as well as spectral properties, the above-mentioned theoretical efforts on the electronic structures, trend in DNA-binding affinities as well as spectral properties of this kind of Ru(II) complex are very significant in guiding the design of molecular "light switch" complexes of DNA and the analysis of their action mechanism.

In this paper, three molecular "light switch" complexes $[Ru(phen)_2L]^{2+}$ (L: dppz, taptp, and phehat) **1**–**3** are selected to perform theoretical studies. The first one is the well-known parent complex $[Ru(phen)_2dppz]^{2+}$**1** for comparison, the second one is $[Ru(phen)_2taptp]^{2+}$ **2** with greatly extended conjugate area, the third one is $[Ru(phen)_2phehat]^{2+}$ **3** with N atoms on the ring skeleton of extended main ligand. This paper is mainly focused on theoretically exploring the trend in DNA-binding affinities of this series of Ru(II) complexes. In addition, the singlet MLCT spectra of these complexes are also computed, simulated and explained by the DFT/TDDFT methods.

2. Computational methods

The investigated complexes are shown in Fig. 1. Each complex with C_2 symmetry is composed of Ru(II) atom, one main ligand L (or called intecalative ligand), and two co-ligands (phen). Seventy-seven to eighty-seven atoms are involved in each complex. The DFT-B3LYP method [20–22] and the LanL2DZ basis set (ECP + DZ for Ru atom, D95 for other atoms) [22,38,39] were adopted. The full geometry optimizations were carried out for the electronic singlet ground states of the complexes [40]. Furthermore, the stable configurations of these complexes were confirmed by frequency analysis, in which no imaginary frequency was found for all configurations at the energy minima. In order to perform accurately the UV–Vis spectral computations, the 40 singlet-excited-state energies in vacuo were calculated by the TDDFT method at B3LYP/LanL2DZ level. In addition, the stereo-contour graphs of some related frontier molecular orbitals of the complexes in the ground states were drawn with the MOLDEN v3.7 program [41] based on the computational results. The GAUSSIAN 98 program package (Revision A.11.4) [42] was used for all the calculations.

3. Results and discussion

3.1. Ligand effects on selected bond lengths and bond angles of the complexes

The computational results and experimental data for the selected bond lengths and bond angles of the complexes are shown in Table 1. Some structural characteristics and differences can be seen from Table 1. First, a subtle but detectable difference in the coordination bond lengths of their main ligands can be found, and the order is $Ru–N_m(\mathbf{3}) > Ru–N_m(\mathbf{2}) > Ru–N_m(\mathbf{1})$, whereas those of their co-ligands are the same (0.2107 nm). Second, the mean bond lengths of co-ligand skeletons are the same (0.1405 nm) and near their standard bond length (0.1400 nm). Third, all dihedral angles of main ligands of these complexes are close to ±0.0, or ±180.0, showing that the planarity of main ligands of these complexes are very excellent and thus advantageous to their parallelly intercalating between the adjacent base-pairs of DNA.

Since the reports on the crystal structures of these three complexes have not been found yet, the direct comparison between the computational results and the corre-

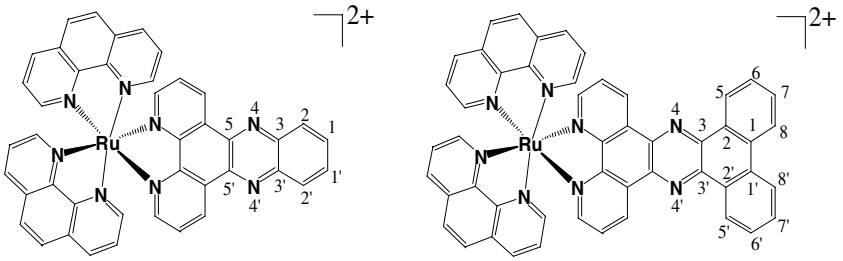

$[Ru(phen)_2(dppz)]^{2+}$ (**1**) $[Ru(phen)_2(taptp)]^{2+}$ (**2**)

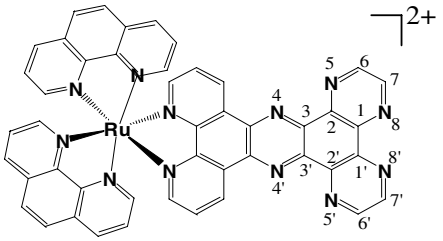

$[Ru(phen)_2(phehat)]^{2+}$ (**3**)

Fig. 1. Structural schematic diagrams and computational models of $[Ru(phen)_2(L)]^{2+}$ (L = dppz, taptp, phehat) **1**–3.

Table 1
Computational selected bond lengths (nm), bond angles (°) and dihedral angles (°) of $[Ru(phen)_2(L)]^{2+}$ (L = dppz, taptp, phehat) **1**–**3** as well as $[Ru(phen)_3]^{2+}$ **0** for comparison

Comp.	Ru–N_m[a]	Ru–N_{co}	C–$C(N)_m$[b]	C–$C(N)_{co}$	A_m[c]	A_{co}	Dihedral angle		
0 (calc)	0.2106	0.2106	0.1405	0.1405	79.5	79.5	–	–	–
$[Ru(phen)_3]^{2+}$(expt)	0.2067	0.2067	–	–	79.9	79.9	–	–	–
1 (L = dppz)	0.2105	0.2107	0.1405	0.1405	79.2	79.4	180.0/180.0 (C1–C2–C3–N4)/ (C1′–C2′–C3′–N4′)	180.0/180.0 (C2–C3–N4–C5)/ (C2′–C3′–N4′–C5)	0.0/−180.0 (C2–C3–C3′–C2″)/ (C2–C3–C3′–N4′)
2 (L = taptp)	0.2106	0.2107	0.1410	0.1405	79.3	79.4	−179.9/−179.9 (C1–C2–C3–N4)/ (C1′–C2′–C3′–N4′)	0.0/0.0 (C1–C2–C5–C6)/ (C1′–C2′–C5′–C6′)	0.0/0.0 (C2–C1–C7–C8)/ (C2′–C1′–C7′–C8′)
3(L = phehat)	0.2108	0.2107	0.1398	0.1405	79.3	79.4	−180.0/−180.0 (C1–C2–C3–N4)/ (C1′–C2′–C3′–N4′)	−0.0/−0.0 (C1–C2–N5–C6)/ (C1′–C2′–N5′–C6′)	0.0/0.0 (C2–C1–C7–N8)/ (C2′–C1′–C7′–N8′)

[a] Ru–N_m expresses the mean coordination bond length between Ru and N atoms of the main ligand (L = dppz, taptp, phehat), and Ru–N_{co} expresses that between Ru and N atoms of the co-ligand (phen).
[b] C–$C(N)_m$ expresses the mean bond length of ring skeleton of the main ligand.
[c] A_m expresses the coordination bond angle between Ru and two N atoms of the main ligand.

sponding experimental data cannot be performed. However, according to the comparison between the calculated results and experimental data of the parent complex $[Ru(phen)_3]^{2+}$ [43] as well as the similar comparison reported by Fantacci et al. [34], we can reasonably deduce that the results of the full geometry optimization computations by the DFT method should be reliable. Therefore, based on the computed geometries of the complexes, we can further perform the studies on the electronic structures, and the trend in DNA-binding affinities and spectral properties of complexes $[Ru(phen)_2(L)]^{2+}$(L = dppz, taptp, phehat).

3.2. Characteristic of the electronic structures of the complexes and their difference

The components and energies of the frontier molecular orbitals are very important to investigate the trend in DNA-binding of complexes and their spectral properties. The stereo contour graphs of the some frontier molecular orbitals of the complexes are also shown in Fig. 2.

From Fig. 2, we can see that: although the component-characteristics of the frontier molecular orbitals of these complexes are similar to those of some other Ru(II) polypyridyl complexes [44,45], there are still some important

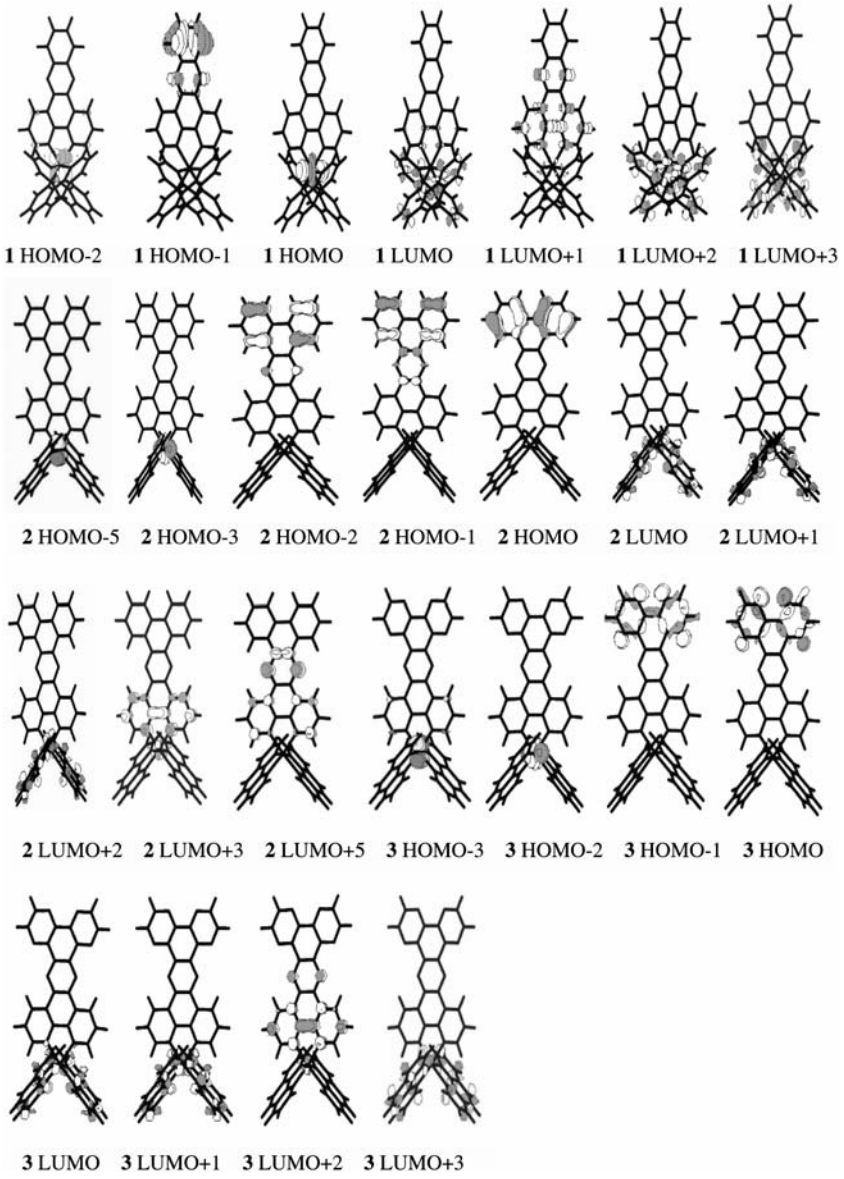

Fig. 2. Some related frontier MOs contour plots of complexes $[Ru(phen)_2(L)]^{2+}$ (L = dppz, taptp, phehat) using the DFT method at the B3LYP/LanL2DZ level.

difference among those of the three complexes. First, the molecular orbitals of which the components come mainly from d orbitals of the central metal atom (Ru) or are characterized by d orbitals of the metal atom, are the HOMO and HOMO-2 for complex **1**, the HOMO-3 for complex **2**, and the HOMO-2 for complex **3**. Second, the molecular orbitals of which the components come mainly from p orbitals of C and N atoms in main-ligand (L), are the LUMO + 1 for complex **1**, the LUMO + 3 for complex **2** and the LUMO + 2 for complex **3**. Such component-characteristics of the frontier molecular orbitals can be used to explain the trend in DNA-binding and spectral properties of these complexes along with their orbital energy characteristics.

The schematic diagram of the computed energies of some frontier molecular orbitals and the related energy transitions of the complexes are shown in Fig. 3. From Fig. 3, we can see that the order of the LUMO energies (ε_{LUMO}) of these complexes is $\varepsilon_{LUMO}(\mathbf{2}) > \varepsilon_{LUMO}(\mathbf{3}) > \varepsilon_{LUMO}(\mathbf{1})$, and the orders of their some LUMO + x energies (ε_{LUMO+x}) are similar to that of their LUMO energies (ε_{LUMO}).

3.3. Trend in DNA-binding affinities

Based on spectroscopic methods, the intrinsic binding constants K_b of the complexes to calf thymus (CT) DNA have been experimentally measured [6,17,18,46–48], shown in Table 2. We can see that the trend in DNA-binding constants (K_b) of this series of complexes is $K_b(\mathbf{2}) < K_b(\mathbf{3}) < K_b(\mathbf{1})$. Such a trend can be reasonably explained by the DFT calculations.

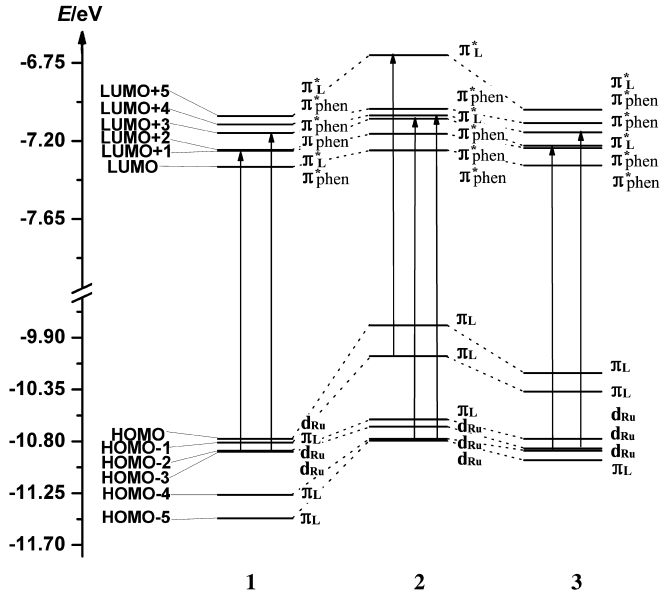

Fig. 3. Schematic diagram of the energies of some frontier MOs of $[Ru(phen)_2(L)]^{2+}$ (L = dppz, taptp, phehat) **1**–**3** using the DFT at the B3LYP/LanL2DZ level (Allowheads express some transitions most contributing to experimental ^{1}MLCT bands (400–500 nm) with the TDDFT method, seeing Table 3).

Table 2
Absorption spectra and DNA-binding constants K_b of $[Ru(phen)_2(L)]^{2+}$(L = dppz, taptp, phehat) 1–3 as well as related references

Complex	Absorption λ_{max} (nm)	K_b (M^{-1})	Ref.
1	439	5.1×10^6(>10^6)	[6,47]
2	465	6.4×10^4	[17]
3	440	2.5×10^6	[18]

It is well known that there are π–π stacking interactions in the DNA-binding of Ru(II) polypyridyl-type complexes in an intercalative (or partly intercalative) mode [4]. Furthermore, many theoretical studies have shown that a DNA molecule is an electron–donor and an intercalated complex is an electron–acceptor [23,49]. For example, based on the DFT calculations and the frontier molecular orbital theory, Reha and Hobza et al.reported that all isolated intercalators (ethidium, daunomycin, ellipticine and 4′,6-diaminide-2-phenylindole) binding to DNA are good electron acceptors because their LUMO energies are almost negative, whereas all isolated bases and base pairs of DNA (e.g., adenine, thymine, and adenine-thymine) are very poor electron acceptors because their LUMO energies are all positive [49]. Kurita and Kobayashi further reported the DFT results for stacked DNA-base-pairs with backbones [23]. Their results indicate that the HOMO energy and the energies of some occupied orbitals near the HOMO are rather high, and the HOMO and HOMO-1 are predominately distributed on the base pairs of DNA, and thus such facts show the bases and base-pairs being good electron donors. Recently, we reported some DFT results on the electronic structures and the trend in DNA-binding affinities of complexes $[Ru(bpy)_2L]^{2+}$ (L = *o*-npip, *m*-npip and *p*-npip) [26], $[RuL_2(pmip)]^{2+}$ (L = bpy, phen, dmp) [50], $[Ru(phen)_2(6\text{-R-dppz})]^{2+}$ (*R* = –OH and –NO_2) [51] and so forth, further supported the above proposals.

Therefore, the factors affecting DNA-binding affinities of the complexes can be usually considered from the planarity, the energy and population of the lowest unoccupied molecular orbital (LUMO, even and LUMO + *x*) of the complex molecule [44,50–52]. The above-mentioned trend in DNA-binding, i.e., $K_b(\mathbf{2}) < K_b(\mathbf{3}) < K_b(\mathbf{1})$, can be explained as follows: the planarities of these complexes are all very excellent and substantially the same, and they all can easily intercalate between base-pairs of DNA in an intercalative mode, so that the key factors affecting K_b are the energies and populations of LUMOs (even and LUMO + *x*) of the complexes. From Fig. 3, we can see that the LUMO energies (ε_{LUMO}) follow the sequence of $\varepsilon_{LUMO}(\mathbf{2})$ (−7.254 eV) > $\varepsilon_{LUMO}(\mathbf{3})$ (−7.341 eV) > $\varepsilon_{LUMO}(\mathbf{1})$ (−7.349 eV). Moreover, from Figs. 2 and 3, we can also see that the LUMO + *x* on which the π-components of intercalative ligands are predominantly populated, are the LUMO + 1 for complex **1**, the LUMO + 3 for complex **2**, the LUMO + 2 for complex **3**, respectively, and their energy order is also $\varepsilon_{LUMO+3}(\mathbf{2})$ (−7.053 eV) > $\varepsilon_{LUMO+2}(\mathbf{3})$ (−7.227 eV) > $\varepsilon_{LUMO+1}(\mathbf{1})$ (−7.257 eV). Synthetically, the two energy orders all lead to the DNA-binding order being $K_b(\mathbf{2}) < K_b(\mathbf{3}) < K_b(\mathbf{1})$, because the lower LUMO and LUMO + *x* energies are advantageous to accepting the electrons of HOMO from DNA-base-pairs in an intercalative mode, based on the frontier molecular orbital theory [53,54]. Therefore, considering the LUMO (even and LUMO + *x*) energies and its π-components on intercalative ligands, the DNA-binding affinity of complex **1** being greater than that of complex **2** and **3** can be explained. On the other hand, the fact that the DNA-binding affinity of complex **3** is greater than that of complex **2** can also be explained by $\varepsilon_{LUMO}(\mathbf{2}) > \varepsilon_{LUMO}(\mathbf{3})$ and $\varepsilon_{LUMO+3}(\mathbf{2}) > \varepsilon_{LUMO+2}(\mathbf{3})$ whereas the planar area of their intercalative ligands is the same.

3.4. Singlet MLCT spectra

The experimental spectra of these Ru(II) complexes in aqueous solution shows the presence of the band of comparable intensity, centered at ca. 400–500 nm, and such a band is generally assigned to a singlet metal-to-ligand charge transfer (^{1}MLCT) in the UV–Vis region and it is very widely applied in bio-inorganic chemistry [10,40]. The spectral properties of the complexes in vacuo have been computed by the TDDFT method at the B3LYP/LanL2DZ level, and the property of ^{1}MLCT bands will be emphatically discussed. The comparison between computational and experimental [17,18,46–48] absorption-spectral data, the related transfers and assignments of ^{1}MLCT spectra of $[Ru(phen)_2(L)]^{2+}$(L = dppz,

taptp, phehat) are further given in Table 3, considering the theoretical transitions characterized by an oscillator strength (f) larger than 0.05 and an orbital contribution larger than 10% within 400–500 nm. The experimental electronic absorption spectra [17,18,48] of complexes **1**–**3** and their simulated ones in the range of 350–550 nm using the TDDFT method in vacuo are also shown in Fig. 4.

From Table 3, we find that for complex **1**, two strong transitions with $f > 0.09$ lie in the range of 400–500 nm. The strongest band ($f = 0.165$) at 424 nm mainly involves the transition from d_{Ru} (HOMO-2) to π^*_L (LUMO + 1) (49%), and it can be characterized by $d_{Ru} \rightarrow \pi^*_L$. Besides this transition most contributing to the strongest band, several transitions with the charter of $d_{Ru} \rightarrow \pi^*_{phan}$, i.e., HOMO → LUMO + 3 (14%), HOMO-2 → LUMO (14%) and HOMO-3 → LUMO + 2 (10%), are involved. The next strongest band at 405 ($f = 0.098$) nm has also an obvious ^{1}MLCT character, and mainly originates from the transition of HOMO-2 → LUMO + 3 (68%) and involves the transition of HOMO → LUMO + 4 (11%). Both of them are characterized by $d_{Ru} \rightarrow \pi^*_{phen}$. Therefore, the experimental broad band of complex **1** at 439 nm can be assigned to a superposition of these two bands with ^{1}MLCT feature. Moreover, considering that the most important contribution to this experimental broad is the transition from d_{Ru} (HOMO-2) to π^*_L (LUMO + 1), the ^{1}MLCT band at 439 nm can be simply assigned to the transition of $d_{Ru} \rightarrow \pi^*_L$.

The strongest band of complex **2** at 424 nm ($f = 0.478$) mainly involves the transitions of HOMO-1 → LUMO + 5 (49%) and HOMO-5 → LUMO + 3 (19%), and thus it can be characterized by $\pi_L \rightarrow \pi^*_L$ and $d_{Ru} \rightarrow \pi^*_L$, respectively. In particular, the next stronger bands at 479 nm ($f = 0.054$), 438 nm ($f = 0.051$) and 419 nm ($f = 0.056$), which are mainly characterized by $d_{Ru} \rightarrow \pi^*_{phen}$, and have an obvious ^{1}MLCT character. Moreover, the next strongest band at 406 nm ($f = 0.091$), has an obvious ^{1}MLCT character, and mainly originates from HOMO-5 → LUMO + 2 (68%) ($d_{Ru} \rightarrow \pi^*_{phen}$). Therefore, the experimental broad band of complex **2** at 465 nm can be also mainly assigned to a superposition of these five calculated bands, and can be assigned to the ^{1}MLCT transition of $d_{Ru} \rightarrow \pi^*_L/\pi^*_{phen}$ with some $\pi_L \rightarrow \pi^*_L$ feature.

The strongest band of complex **3** at 426 nm ($f = 0.201$) mainly involves the transition of the HOMO-3 → LUMO + 2 (53%), and thus it can be mainly characterized by $d_{Ru} \rightarrow \pi^*_L$. The next strongest band at 406 ($f = 0.088$) nm, has also an obvious ^{1}MLCT character, and mainly originates from HOMO-3 → LUMO + 3 (57%) ($d_{Ru} \rightarrow \pi^*_{phen}$). Therefore, the experimental broad band (440 nm) of complex **3** can be assigned to a superposition of these two bands, moreover, the most important contribution to this experimental band is the transition from d_{Ru} (HOMO-3) to π^*_L (LUMO + 2), and thus it can be simply assigned to the transition of $d_{Ru} \rightarrow \pi^*_L$.

In summary, the experimental singlet metal-to-ligand charge transfer (^{1}MLCT) bands of this series of complexes

Table 3
Comparison between computational and experimental [6,17,18] wave lengths (λ_{max}) of ^{1}MLCT absorption spectra of $[Ru(phen)_2(L)]^{2+}$ (L = dppz, taptp, phehat) **1**–**3** as well as their assignments using the TDDFT at the B3LYP/LanL2DZ level

No	Wavelength (nm)			Assignment		
	Expt	Calc	f[a]			
1	439	426	0.165	HOMO-2 → LUMO + 1 (49%)[b]	$d_{Ru} \rightarrow \pi^*_L$	b → b[c]
				HOMO → LUMO + 3 (14%)	$d_{Ru} \rightarrow \pi^*_{phen}$	a → a
				HOMO-2 → LUMO (14%)	$d_{Ru} \rightarrow \pi^*_{phen}$	b → b
				HOMO-3 → LUMO + 2 (10%)	$d_{Ru} \rightarrow \pi^*_{phen}$	a → a
		405	0.098	HOMO-2 → LUMO + 3 (68%)	$d_{Ru} \rightarrow \pi^*_{phen}$	b → a
				HOMO → LUMO + 4 (11%)	$d_{Ru} \rightarrow \pi^*_{phen}$	a → b
2	465	479	0.054	HOMO-1 → LUMO + 3 (70%)	$\pi_L \rightarrow \pi^*_L$	b → b
		438	0.051	HOMO-4 → LUMO (42%)	$d_{Ru} \rightarrow \pi^*_{phen}$	a → b
				HOMO-5 → LUMO + 1 (27%)	$d_{Ru} \rightarrow \pi^*_{phen}$	b → a
				HOMO-3 → LUMO + 4 (13%)	$d_{Ru} \rightarrow \pi^*_{phen}$	a → b
		424	0.478	HOMO-1 → LUMO + 5 (49%)	$\pi_L \rightarrow \pi^*_L$	b → b
				HOMO-5 → LUMO + 3 (19%)	$d_{Ru} \rightarrow \pi^*_L$	b → b
		419	0.056	HOMO-3 → LUMO + 4 (56%)	$d_{Ru} \rightarrow \pi^*_{phen}$	a → b
				HOMO-5 → LUMO + 3 (17%)	$d_{Ru} \rightarrow \pi^*_L$	b → b
		406	0.091	HOMO-5 → LUMO + 2 (68%)	$d_{Ru} \rightarrow \pi^*_{phen}$	b → a
3	440	426	0.201	HOMO-3 → LUMO + 2 (53%)	$d_{Ru} \rightarrow \pi^*_L$	b → b
				HOMO-2 → LUMO + 3 (14%)	$d_{Ru} \rightarrow \pi^*_{phen}$	a → a
				HOMO-4 → LUMO + 1 (11%)	$d_{Ru} \rightarrow \pi^*_{phen}$	a → a
				HOMO-3 → LUMO (10%)	$d_{Ru} \rightarrow \pi^*_{phen}$	b → b
		406	0.088	HOMO-3 → LUMO + 3 (57%)	$d_{Ru} \rightarrow \pi^*_{phen}$	b → a
				HOMO-2 → LUMO + 4 (14%)	$d_{Ru} \rightarrow \pi^*_{phen}$	a → b

[a] Oscillator strength.
[b] The percentage contributions to wavefunctions of excited states are given in parenthesis.
[c] The orbital symmetries of the related transitions.

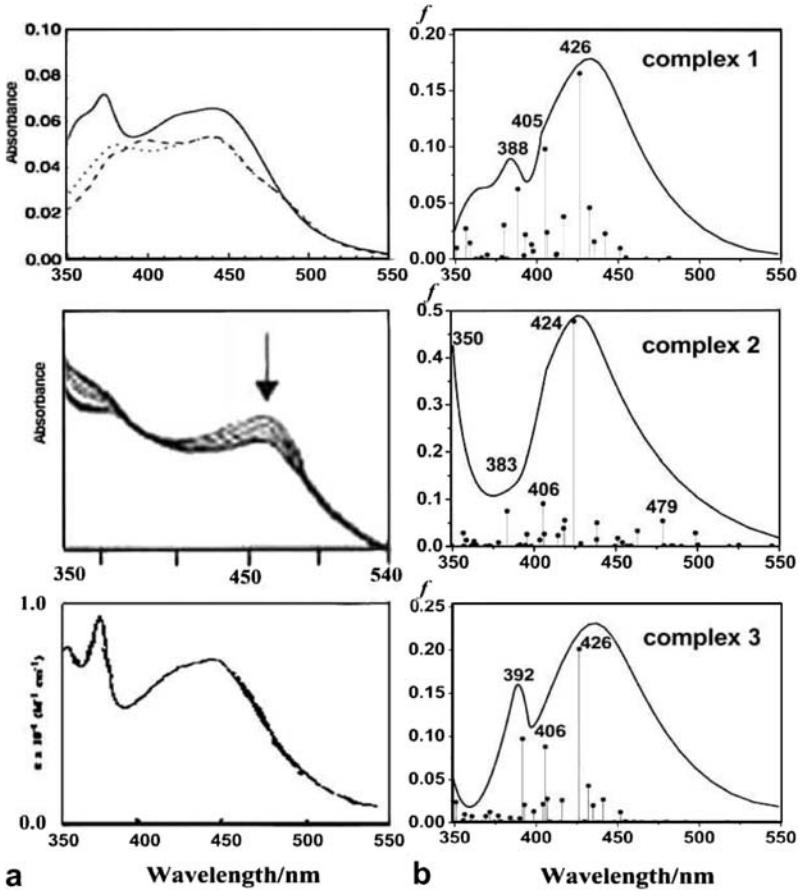

Fig. 4. (a) Electronic absorption spectra of complex **1**–**3** [17,18,47]. For complex **1**: absorption spectra of the Δ-$[Ru(phen)_2(dppz)]^{2+}$ in the absence of DNA (solid curve), in the presence of poly[$d(AT)_2$] (dotted curve), and in the presence of DAPI-poly[$d(A\text{-}T)_2$] (dashed curve) [47]; For complex **2**: the arrowhead expresses the increase in DNA concentration from zero [17]. (b) Corresponding simulated spectra in 300–550 nm and oscillator strengths (*f*) using the TDDFT method in vacuo.

can be minutely discussed by the TDDFT computations. Increasing the planar area of intercalative ligand can make ^{1}MLCT band red-shift and mix with some $\pi_L \rightarrow \pi_L^*$ feature. Introducing N atoms into the ring skeleton of intercalative ligand can make ^{1}MLCT band blue-shift and keep the excellent $d_{Ru} \rightarrow \pi_L^*/\pi_{phen}^*$ feature.

It is interesting to find the following: the excited and accepting orbitals of every transition with the largest *f* value for all these complexes have the same symmetry (b symmetry of C_2 point group) and an excellent overlapping population, as shown in Table 3 and Fig. 2. It means that the same symmetries of the related orbitals must be advantageous to the most effective orbital overlap in the studied system, and thus be advantageous to the related transition. Such a fact is in agreement with a general insight of the radiation theory [55], and thus further shows the above computational results being reliable. In addition, the simulated electronic absorption spectra in the range of 350–550 nm are also presented along with the experimental ones in Fig. 4. The errors of the calculated wavelengths from experiment data for this series of the complexes, lie within 10–30 nm.

In addition, solvent effect may play a role to a limited extent in simulation of the electronic spectra of highly polar solvents and/or solvents with hydrogen bond [34]. Here our limited studies did not perform this rectification. We hope to further investigate these effects in future studies. Even though, the solvatochromism of the Ru(II) complexes are very small [4,52]. Therefore, the gas-phase calculations are still suitable to reproduce the experimental spectra of this kind of Ru(II) complex [24,28,33,34].

4. Conclusions

The DFT study on a series of molecular "light switch" complexes $[Ru(phen)_2L^{2+}$(L = dppz, taptp, phehat) **1**–**3** shows that simply increasing the planar area of intercalative ligand may be ineffective on improvement of DNA-binding of resulting complex because of going with the increase in the LUMO (and LUMO + *x*) energy, but inducing some heteroatoms (e.g., N atom) with stronger electronegativity in the ring skeleton of intercalative ligand should be effective because of the decrease in the LUMO (and LUMO + *x*) energy to a certain extent. Therefore,

the trend in DNA-binding constants (K_b) of this series of the complexes, i.e., $K_b(\mathbf{2}) < K_b(\mathbf{3}) < K_b(\mathbf{1})$, which is closely related to the luminescence property of the complex in DNA, can be reasonably explained. In addition, the ^{1}MLCT spectra of this series of complexes can be minutely discussed by the TDDFT calculations, and it is interesting to find that the symmetries of the excited and accepting orbitals of the transition with the largest f value are the same. It means that the same symmetries of the related orbitals must be advantageous to the most effective orbital overlap in the studied system, and thus advantageous to the related transition.

Acknowledgements

The financial supports of the National Natural Science Foundation of China, the Natural Science Foundation of Guangdong Province and the Research Fund for the Doctoral Program of Higher Education of China are gratefully acknowledged.

References

[1] J.K. Barton, Science 233 (1986) 727.
[2] B. Nordén, P. Lincoln, B. Åkerman, E. Tuite, Met. Ions Biol. Syst. 33 (1996) 177.
[3] P.M. Takahara, A.C. Rosenzweig, C.A. Frederick, S.J. Lippard, Nature 377 (1995) 649.
[4] L.N. Ji, J.G. Liu, X.H. Zou, Coord. Chem. Rev. 513 (2001) 216.
[5] P. Nordell, P. Lincoln, J. Am. Chem. Soc. 127 (2005) 9670.
[6] R.M. Hartshorn, J.K. Barton, J. Am. Chem. Soc. 114 (1992) 5919.
[7] A.E. Friedman, J.C. Chambron, J.P. Sauvage, N.J. Rurron, J.K. Barton, J. Am. Chem. Soc. 112 (1990) 4960.
[8] Y. Jenkins, A.E. Friedman, N.J. Turro, J.K. Barton, Biochemistry 31 (1992) 10809.
[9] P.Y. Chen, T.J. Meyer, Chem. Rev. 98 (1998) 1439.
[10] E.J.C. Olsen, D. Hu, A. Hörmann, M.R. Arkin, E.D.A. Stemp, J.K. Barton, P.F. Barbara, J. Am. Chem. Soc. 119 (1997) 11458.
[11] R.B. Nair, B. Cullum, C.J. Murphy, Inorg. Chem. 36 (1997) 962.
[12] J. Olofsson, B. Onfelt, B. Lincoln, B. Norden, P. Matousek, A.W. Parker, E. Tuite, J. Inorg. Biochem. 91 (2002) 286.
[13] M.K. Brennaman, T.J. Meyer, J.M. Papanikolas, J. Phys. Chem. A 108 (2004) 9938.
[14] J. Olofsson, L.M. Wilhelmsson, P. Lincoln, J. Am. Chem. Soc. 126 (2004) 15458.
[15] S. Arounaguiri, B.G. Maiya, Inorg. Chem. 38 (1999) 842.
[16] K.A. O'Donoghue, J.M. Kelly, P.E. Kruger, J. Chem. Soc., Dalton. Trans. (2004) 13.
[17] Q.X. Zhen, B.H. Ye, J.G. Liu, Q.L. Zhang, L.N. Ji, L. Wang, Inorg. Chim. Acta 303 (2000) 141.
[18] C. Moucheron, A. Kirsch-De Mesmaeker, S. Choua, Inorg. Chem. 36 (1997) 584.
[19] J.G. Liu, B.H. Ye, H. Chao, Q.X. Zhen, L.N. Ji, Chem. Lett. (1999) 1085.
[20] P. Hohenberg, W. Kohn, Phys. Rev. B 136 (1964) 864.
[21] A.D. Becke, J. Chem. Phys. 98 (1993) 1372.
[22] J.B. Foresman, M.J. Frisch, Exploring Chemistry with Electronic Structure Methods, second ed., Gaussian Inc, Pittsburgh, PA, 1996.
[23] N. Kurita, K. Kobayashi, Comput. Chem. 24 (2000) 351.
[24] S.I. Gorelsky, A.B.P. Lever, J. Organomet. Chem. 635 (2001) 187.
[25] K.C. Zheng, J.P. Wang, W.L. Peng, X.W. Liu, F.C. Yun, J. Phys. Chem. A 105 (2001) 10899.
[26] S. Shi, J. Liu, J. Li, K.C. Zheng, C.P. Tan, L.M. Chen, L.N. Ji, J. Chem. Soc., Dalton. Trans. (2005) 2038.
[27] X.W. Liu, J. Li, K.C. Zheng, Z.W. Mao, L.N. Ji, Inorg. Chim. Acta 358 (2005) 3311.
[28] J. Li, L.C. Xu, J.C. Chen, K.C. Zheng, L.N. Ji, J. Phys. Chem. A 110 (2006) 8174.
[29] A. Dreuw, B.D. Dunietz, M. Head-Gordon, J. Am. Chem. Soc. 124 (2002) 12070.
[30] A. Tsolakidis, E. Kaxiras, J. Phys. Chem. A 109 (2005) 2373.
[31] A. Dreuw, M. Head-Gordon, J. Am. Chem. Soc. 126 (2004) 4007.
[32] A. Dreuw, M. Head-Gordon, Chem. Rev. 105 (2005) 4009.
[33] X. Zhou, A.M. Ren, J.K. Feng, J. Organomet. Chem. 690 (2005) 338.
[34] S. Fantacci, F. De Angelis, A. Sgamellotti, N. Re, Chem. Phys. Lett. 396 (2004) 43.
[35] G. Pourtois, D. Beljonne, C. Moucheron, S. Schumm, A.K. Mesmaeker, R. Lazzaroni, J.L. Bredas, J. Am. Chem. Soc. 126 (2004) 683.
[36] E.R. Batista, R.L. Martin, J. Phys. Chem. A 109 (2005) 3028.
[37] S. Fantacci, F. De Angelis, A. Sgamellotti, A. Marrone, N. Re, J. Am. Chem. Soc. 127 (2005) 14144.
[38] P.J. Hay, W.R. Wadt, J. Chem. Phys. 82 (1985) 270.
[39] W.R. Wadt, P.J. Hay, J. Chem. Phys. 82 (1985) 284.
[40] A. Juris, V. Balzani, F. Barigelletti, S. Campagna, P. Belser, A. von Zelewsky, Coord. Chem. Rev. 84 (1988) 85.
[41] G. Schaftenaar, J.H. Noordik, J. Comput. Aided. Mol. Des. 14 (2000) 123.
[42] M.J. Frisch, G.W. Trucks, H.B. Schlegel, G.E. Scuseria, M.A. Robb, J.R. Cheeseman, V.G. Zakrzewski, J.A. Montgomery Jr., R.E. Stratmann, J.C. Burant, S. Dapprich, J.M. Millam, A.D. Daniels, K.N. Kudin, M.C. Strain, O. Farkas, J. Tomasi, V. Barone, M. Cossi, R. Cammi, B. Mennucci, C. Pomelli, C. Adamo, S. Clifford, J. Ochterski, G.A. Petersson, P.Y. Ayala, Q. Cui, K. Morokuma, N. Rega, P. Salvador, J.J. Dannenberg, D.K. Malick, A.D. Rabuck, K. Raghavachari, J.B. Foresman, J. Cioslowski, J.V. Ortiz, A.G. Baboul, B.B. Stefanov, G. Liu, A. Liashenko, P. Piskorz, I. Komaromi, R. Gomperts, R.L. Martin, D.J. Fox, T. Keith, M.A. Al-Laham, C.Y. Peng, A. Nanayakkara, M. Challacombe, P.M.W. Gill, B. Johnson, W. Chen, M.W. Wong, J.L. Andres, C. Gonzalez, M. Head-Gordon, E.S. Replogle, J.A. Pople, GAUSSIAN 98, Revision A.11.4, Gaussian, Inc., Pittsburgh, PA, 2002.
[43] D.J. Maloney, F.M. MacDonnell, Acta Crystallogr., Sect. C 53 (1997) 705.
[44] W.J. Mei, J. Liu, K.C. Zheng, L.J. Lin, H. Chao, A.X. Li, F.C. Yun, L.N. Ji, J. Chem. Soc., Dalton. Trans. (2003) 1352.
[45] K.C. Zheng, H. Deng, X.W. Liu, H. Li, H. Chao, L.N. Ji, J. Mol. Struct. Theochem. 682 (2004) 225.
[46] I. Haq, P. Lincoln, D. Suh, B. Norden, B.Z. Chowdhry, J.B. Chaires, J. Am. Chem. Soc. 117 (1995) 4788.
[47] B.N. Rajesh, S.T. Emily, L.K. Shalawn, J.M. Catherine, Inorg. Chem. 37 (1998) 139.
[48] B.H. Yun, J.O. Kim, B.W. Lee, P. Lincoln, B. Norden, J.M. Kim, S.K. Kim, J. Phys. Chem. B 107 (2003) 9858.
[49] D. Řeha, M. Kabeláč, F. Ryjáček, J. Šponer, J.E. Šponer, M. Elstner, S. Suhai, P. Hobza, J. Am. Chem. Soc. 124 (2002) 3366.
[50] H. Xu, K.C. Zheng, H. Deng, L.J. Lin, Q.L. Zhang, L.N. Ji, New J. Chem. 27 (2003) 1255.
[51] X.W. Liu, J. Li, K.C. Zheng, H. Chao, L.N. Ji, J. Inorg. Biochem. 99 (2005) 2372.
[52] S. Shi, J. Liu, J. Li, K.C. Zheng, C.P. Tan, L.M. Chen, L.N. Ji, J. Inorg. Biochem. 100 (2006) 385.
[53] K. Fukui, T. Yonezawa, H. Shingu, J. Chem. Phys. 20 (1952) 722.
[54] I. Fleming, Frontier Orbital and Organic Chemical Reaction, Wiley, New York, 1976.
[55] R.A. Marcus, Rev. Mod. Phys. 65 (1993) 599.